Available online at www.sciencedirect.com
ScienceDirect
Journal of Energy Chemistry 23(2014)513–518
JOURNAL OF ENERGY CHEMISTRY
www.elsevier.com/journals/journal-of-energy-chemistry/2095-4956
www.elsevier.com/locate/jngc

Nano-crystalline FeOOH mixed with SWNT matrix as a superior anode material for lithium batteries

Mingzhong Zou[a], Weiwei Wen[a], Jiaxin Li[a,b], Yingbin Lin[a], Heng Lai[a*], Zhigao Huang[a*]

a. College of Physics and Energy, Fujian Normal University, Fuzhou 350007, Fujian, China;
b. State Key Laboratory of Structural Chemistry, Fujian Institute of Research on the Structure of Matter, Chinese Academy of Sciences, Fuzhou 350002, Fujian, China

[Manuscript received January 7, 2014; revised February 25, 2014]

Abstract

Nano-crystalline FeOOH particles (5∼10 nm) have been uniformly mixed with electric matrix of single-walled carbon nanotubes (SWNTs) for forming FeOOH/SWNT composite via a facile ultrasonication method. Directly using the FeOOH/SWNT composite (containing 15 wt% SWNTs) as anode material for lithium battery enhances kinetics of the Li^+ insertion/extraction processes, thereby effectively improving reversible capacity and cycle performance, which delivers a high reversible capacity of 758 $mAh{\cdot}g^{-1}$ under a current density of 400 $mA{\cdot}g^{-1}$ even after 180 cycles, being comparable with previous reports in terms of electrochemical performance for FeOOH anode. The good electrochemical performance should be ascribed to the small particle size and nano-crystalline of FeOOH, as well as the good electronic conductivity of SWNT matrix.

Key words

FeOOH/SWNT composite; electrochemical properties; energy storage; lithium batteries; anode material

1. Introduction

Developing the new anode materials via facile routes is a key to develop the next-generation lithium ion batteries (LIBs) [1−3]. Metal oxides and metal oxyhydroxides, especially FeOOH provided with a large theoretical capacity of 905 $mAh{\cdot}g^{-1}$, low cost and environmental friendliness, have been investigated as alternative anode materials to the commercial graphite anode [4−13]. However, rapid capacity decay resulted from the specific volume change, and low electronic conductance of FeOOH materials extremely limits their potential application [11−13]. Researchers mainly focus on controlling the crystalline phase [14,15], synthesizing new nanostructures [11,12,16], or utilizing carbonaceous materials as buffer carriers for addressing those problems [13]. For example, Funabiki et al. and Jain et al. have reported that reducing the crystallization of FeOOH provided with good conductance can improve its cycling performance [14,15]. But until now, most FeOOH anodes were cycled less than several decades of times and always suffer from capacity fading at high current densities [11−13]. Thus, good electrochemical performance including cycling stabilities and rate capacities for FeOOH anodes needs to be achieved, especially at a high rate. According to the diffusion formula $t = L^2/2D$ (where t is the time constant for Li^+ and e^- insertion/extraction into/from the active particles, L is the diffusion length, and D is the diffusion coefficient), reducing the particle size can significantly shorten the diffusion time of Li^+ in active materials, resulting in a much enhanced electrochemical performance [17,18]. Thus, how to use a simple method for simultaneously solving three above-mentioned problems such as to reduce the size of active material, to obtain the applicable crystalline structure and to improve the conductance, has been a major challenge for FeOOH materials used as high performance anodes in LIBs.

In this work, nano-crystalline FeOOH particles (5∼10 nm) have been synthesized via a wet chemical method. And the FeOOH particles have been further mixed with SWNTs matrix for forming uniform FeOOH/SWNT composite. The electrochemical analysis reveals that the FeOOH/SWNTs can afford an obviously better electrochemical performance compared to the pure FeOOH, with a high reversible capacity of 758 $mAh{\cdot}g^{-1}$ even after 180 cycles under a relatively high current density of 400 $mA{\cdot}g^{-1}$. Additionally, this facile approach is suitable for boosting the electrochemical properties of anode materials for LIBs.

* Corresponding author. Tel/Fax: +86-591-22867577; E-mail: zghuang@fjnu.edu.cn; Tel/Fax: +86-591-22867577; E-mail: laiheng@fjnu.edu.cn
This work was supportted by the Natural Science Foundations of China (No.21203025, No. 11004032 and No.11074039).

doi: 10.1016/S2095-4956(14)60179-0

2. Experimental

2.1. Materials synthesis and characterization

All chemicals were of analytical grade and were used as received. The details for the preparation of the SWNTs were presented in our earlier work [19]. Briefly, a single process was adopted to prepare FeOOH NPs. 0.60 mmol phenylphosphonic acid and 0.60 mmol $Fe(NO_3)_3{\cdot}9H_2O$ were dispersed in de-ionized water and sonicated to form homogeneous solution. About 30 mL $NaBH_4$ (0.20 mol/L) solution was added drop by drop and the mixtures were stirred for 30 min. The final product of FeOOH NPs was filtered and washed several times with de-ionized water, and then dried at 80 °C overnight. Then, 85 mg FeOOH NPs have been mixed with 15 mg SWNTs in sodium dodecyl sulfate solution and sonicated for 1 h. The obtained solution was filtered and washed several times with de-ionized water, and then dried at 80 °C overnight for forming the FeOOH/SWNT composites (as shown in Scheme 1). The samples were characterized by scanning electron microscope (SEM), transmission electron microscope (TEM) and X-ray diffraction (XRD).

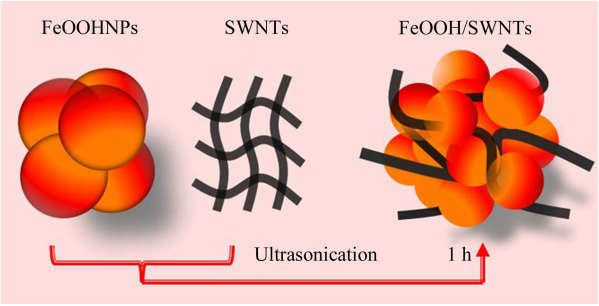

Scheme 1. Schematic one-step synthesis of FeOOH/SWNT composites

2.2. Electrode assembly and measurement

The electrochemical behaviors were measured via CR2025 coin-type test cells assembled in a dry argon-filled glove box. The test cell consisted of working electrode ($\sim$2.0 mg·cm^{-2}) and lithium sheet which were separated by a Celgard 2300 membrane and electrolyte of 1 mol/L LiPF6 in EC : EMC : DMC (1 : 1 : 1 in volume). For FeOOH, the working electrode consisted of 80 wt% active material, 10 wt% carbon black and 10 wt% polyvinylidene difluoride (PVDF). And for FeOOH/SWNTs, the electrode consisted of 90 wt% active material and 10 wt% PVDF. The capacities of the active material are calculated based on the whole weight of FeOOH/SWNT composites. Cyclic voltammetry tests were operated on a CHI660D electrochemical workstation with a scan rate of 0.50 mV·s^{-1}. The cells were cycled by LAND 2001A at room temperature. Electrochemical impedance measurements were carried out by applying an AC voltage of 5 mV over the frequency range from 1 MHz to 100 kHz.

3. Results and discussion

The SEM image presented in Figure 1(a) reveals that the purified SWNTs as webs of curved nanotubes form strong intertwined entanglements with a network structure. Figure 1(b) shows the morphology of agglomerated FeOOH particles. The FeOOH particles cannot be distinguished from the SEM image, which is due to the small size of their particles. Figure 1(c) and 1(d) shows the corresponding typical TEM images of the SWNTs and pure FeOOH. From Figure 1(c), the SWNTs appear as bundles with part appearing as individuals. As shown in inset of Figure 1(c), the typical diameter of a SWNT is $\sim$1.4 nm and the two parallel dark lines correspond to the SWNT walls. Herein, the SWNT product is of ultrahigh purity ($\sim$99%) [20]. Figure 1(d) shows that the diameter of FeOOH particles is in the range of 5$-$10 nm. The regular interplanar spacing of 0.25 and 0.42 nm for FeOOH particles respectively ascribed to (040) and (110) planes can be observed.

As shown in Scheme 1, the synthesis of the FeOOH/SWNT composite went through a rapid sonication progress using purified SWNTs and FeOOH particles as the starting materials. As disclosed in the SEM image shown in Figure 2(a), the composite consisting of agglomerative FeOOH particles embedded with a SWNT matrix was obtained. The intertwined SWNTs are wrapped around the agglomerated FeOOH particles, showing a good connection between FeOOH particles and SWNT networks. Hereby, the SWNT networks can provide a good electronic conductivity between FeOOH particles. Figure 2(b) shows that the diffraction peaks of the X-ray diffraction pattern of the FeOOH/SWNT composite are in good agreement with the standard values for α-FeOOH (JCPDS card, No.81$-$0464) except for an additional diffraction peak at about 26^o taken from SWNTs. The weak and broad peaks indicate a nanocrystallinity of the FeOOH particles.

The cyclic voltammetry (CV) curves of FeOOH and FeOOH/SWNT electrodes at the first 6 cycles in the voltage window of 3.0$-$0.05 V at a scan rate of 0.5 mV·s^{-1} are shown in Figure 3(a) and 3(b). According to the previous reports [12,13], the cathodic peak around 1.2 V in the 1st cycle shown in Figure 3(a) corresponds to the reaction of $FeOOH+Li^+ + e^- \rightarrow FeOOHLi$. The peak at 0.65 V with a sloping curve down to the cutoff voltage of 0.05 V is attributed to the reaction of $FeOOHLi+2Li^+ + 2e^- \rightarrow Fe^0 + LiOH + Li_2O$ and the formation of the solid electrolyte interface (SEI) layer. The anodic peak presented from 1.5 V to 2.2 V represents the oxidation from Fe^0 to Fe^{3+}. In the subsequent 5 cycles, the 0.65 V reduction peak becomes diminished, indicating that the formation of the SEI layer only takes place during the 1st cycle. Compared to the CV curves of FeOOH shown in

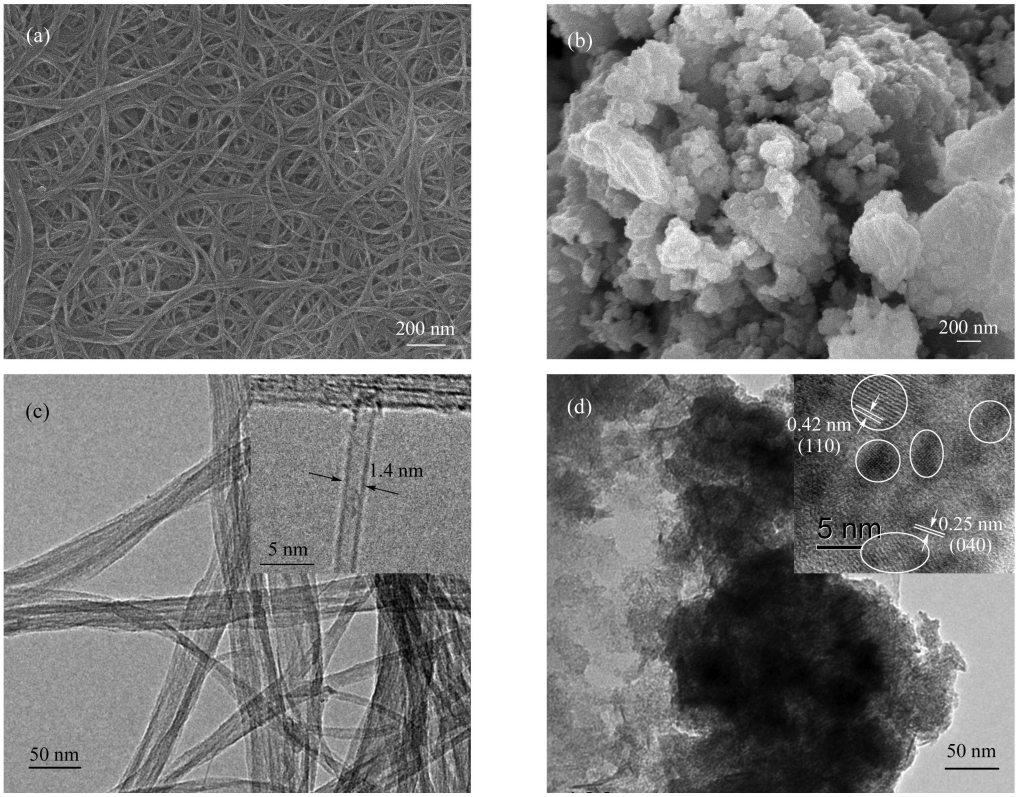

Figure 1. SEM images of (a) SWNTs and (b) FeOOH; TEM and high-resolution TEM images of (c) SWNTs and (d) FeOOH

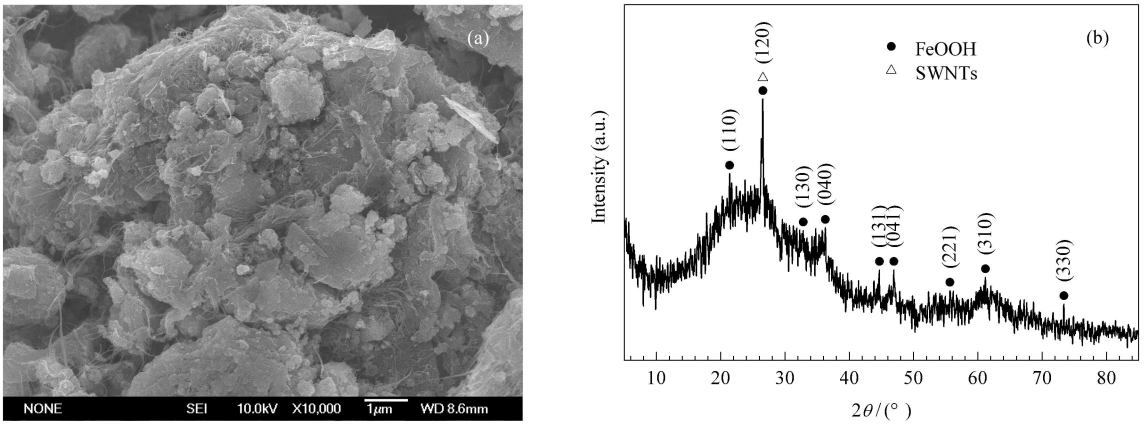

Figure 2. (a) SEM image and (b) XRD pattern of FeOOH/SWNT composite

Figure 3(a), it is observed from Figure 3(b) that the peaks in the following 5 cycles overlap well, indicating a better electrochemical reversibility and structural stability for FeOOH/SWNTs. Moreover, the subsequent redox process may be ascribed to the reversible reaction of $2Fe^0+3Li_2O \rightarrow Fe_2O_3+6Li^++6e^-$ [11]. Accordingly, the discharge/charge (D/C) profiles of the FeOOH and FeOOH/SWNT electrodes in the 1st, 2nd, 10th, 30th and 60th cycles at a current density of 100 $mA \cdot g^{-1}$ between 0.05 V and 3.00 V are presented in Figure 3(c) and 3(d), respectively. Those voltage plateaus shown in D/C curves for the FeOOH and FeOOH/SWNT electrodes are consistent with the CV observation, and being similar to the reported FeOOH anode materials [13]. From Figure 3(c), it is found that the first D/C curves of FeOOH electrode deliver capacities of 1360 and 930 $mAh \cdot g^{-1}$, implying an irreversible capacity loss of ~31%. However, the first D/C capacities for the FeOOH/SWNT electrode were 1340 and 905 $mAh \cdot g^{-1}$, with an larger irreversible capacity loss of ~33% compared to that of FeOOH. This larger capacity loss may result from the additional formation of SEI layer from SWNTs in FeOOH/SWNT composite. In addition, the D/C curves in the 10th, 30th and 50th cycles almost overlapped with the 2nd cycle presented in Figure 3(d), obviously indicating the better cycling performance compared to that of FeOOH electrode shown in Figure 3(c).

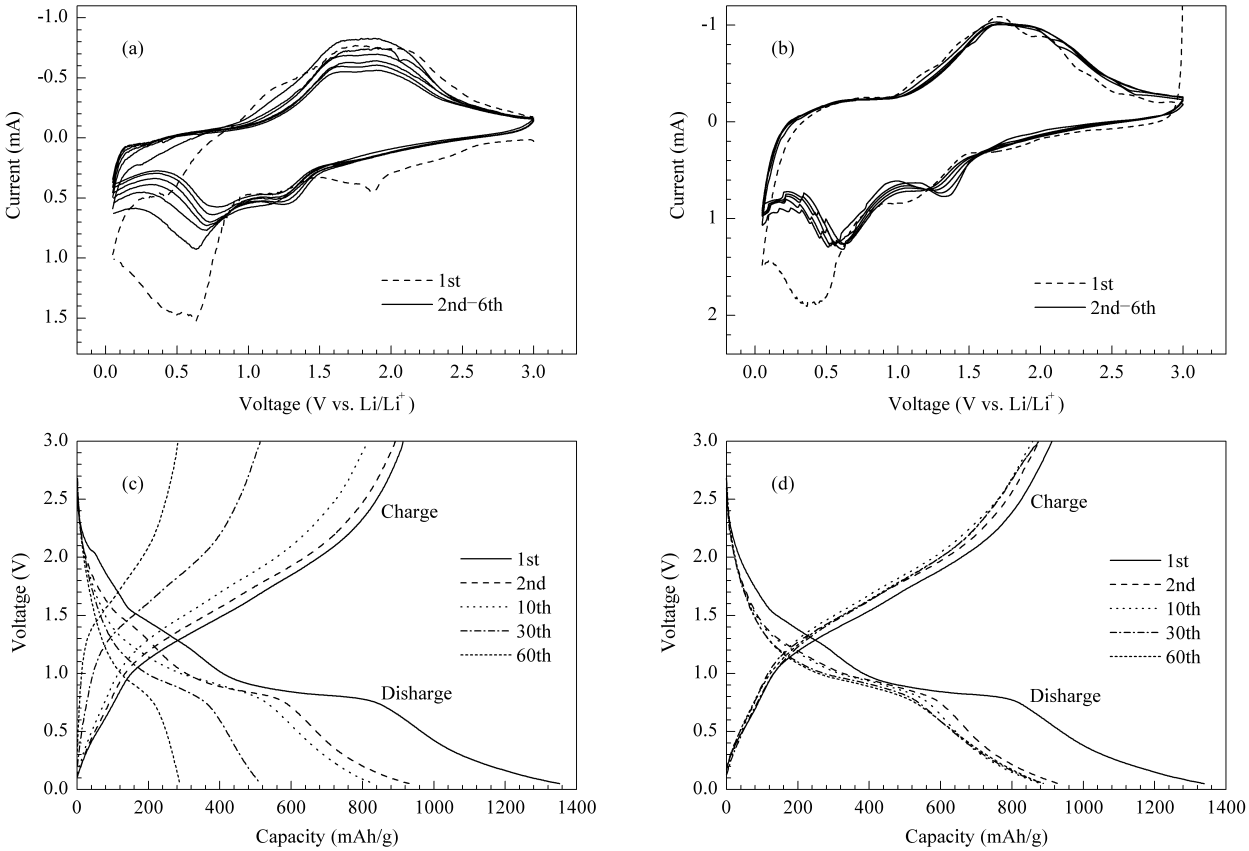

Figure 3. Cyclic voltammetry curves and discharge-charge curves between 0.05 and 3 V (versus Li/Li^+) of Li insertion/extraction into/from the electrodes (a,c) FeOOH and (b,d) FeOOH/SWNT composite

The galvanostatic method was used to estimate the cycle performance of these electrodes. As can be seen from Figure 4(a), the capacity for pure FeOOH electrode decreased with the increasing cycle numbers. The capacity of FeOOH tested at 100 $mA{\cdot}g^{-1}$ was only 295 $mAh{\cdot}g^{-1}$ after 60 cycles. This capacity fading of pure FeOOH could be resulted from its aggregation and pulverization during D/C processes. However, the general properties for pure FeOOH obtained here are still better than the previous report (e.g. 75 $mAh{\cdot}g^{-1}$ at 50th cycle) [13], which could be ascribed to its nano-crystalline structure providing better conductance. After embedding in SWNTs, the specific capacity of FeOOH/SWNT composite can remain at $\sim$840 $mAh{\cdot}g^{-1}$ after 60 cycles, presenting better electrochemical performance than pure FeOOH. To further evaluate the long life cycle performance, the FeOOH/SWNT electrode was cycled under a relatively high current density of 400 $mA{\cdot}g^{-1}$. As shown in Figure 4(b), the reversible specific capacity stabilized at 758 $mAh{\cdot}g^{-1}$ even after 180 cycles. The reversible capacity is much higher than the theoretical capacity of commercial graphite of 372 $mAh{\cdot}g^{-1}$. Meanwhile, the coulombic efficiency of the FeOOH/SWNT electrode after the first 6 cycles kept around $\sim$99% until 180 cycles. The rate performance of the FeOOH/SWNT electrode under various current densities from 100 to 1800 $mA{\cdot}g^{-1}$ is also presented in Figure 4(c). From the Figure 4(c), it is found that the fairly stable capacities at different current densities can be observed. Even at a high rate of 1800 $mAh{\cdot}g^{-1}$, the specific capacity remained at $\sim$400 $mAh{\cdot}g^{-1}$. When the cycling current was reduced back to 100 $mA{\cdot}g^{-1}$, the composite can still deliver a reversible capacity of 780 $mAh{\cdot}g^{-1}$, implying that the structure of the electrode remained stable after various rate cycles. The high capacity, excellent cyclic stability and good rate performance of the FeOOH/SWNT composite could be attributed to the intimate interaction between the nanocrystalline FeOOH particles and the electric SWNT matrix.

Figure 5 shows EIS impedance spectra of FeOOH and FeOOH/SWNT electrodes after test and the corresponding equivalent circuit. EIS impedance spectra are fitted with the corresponding equivalent circuit, where R_e, R_{sf} and R_{ct}, denote the solution resistance, the diffusion resistance of Li ions through SEI layer and the charge-transfer resistance, respectively. R_w is the Warburg impedance. As shown in Table 1, the R_{ct} for FeOOH/SWNT is smaller than that of FeOOH, indicating that the presence of SWNT matrix can improve the electronic-conductivity. To further investigate the electrode kinetics, the diffusion coefficient of Li ions (D_{Li^+}) for FeOOH and FeOOH/SWNT electrodes can be calculated from the following equation [21]:

$$D = \frac{R^2T^2}{2A^2n^4F^4C^2\sigma^2}$$

where, R is the gas constant, T is the absolute temperature, A is the surface area of the cathode, n is the number of electrons per molecule during oxidization, F is the Faraday constant, C is the concentration of lithium ion, and σ is the Warburg factor which obeys the following relationship:

$$Z_{\text{real}} = R_{\text{e}} + R_{\text{ct}} + \sigma\omega^{-1/2}$$

where, R_{e} is the resistance between the electrolyte and electrode, R_{ct} is the charge transfer resistance, and ω is angle frequency.

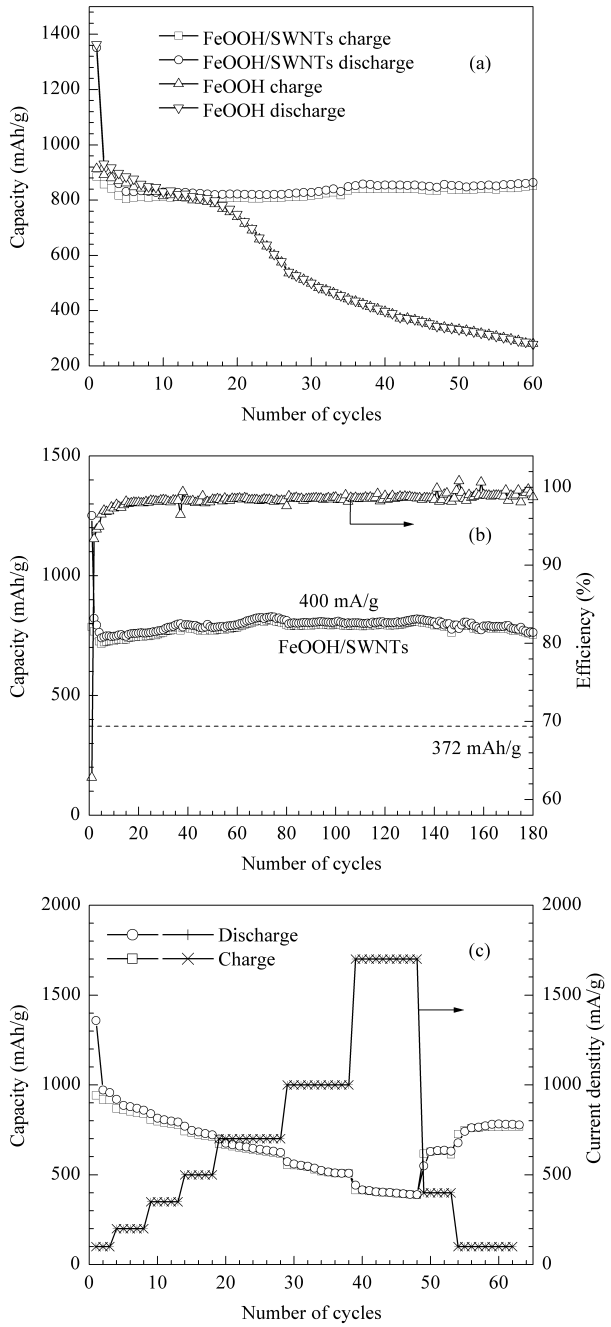

Figure 4. (a) Cycling performance of pure FeOOH and FeOOH/SWNTs electrodes at a current density of 100 mA/g, (b) cycling performance of FeOOH/SWNT electrode at a current density of 400 mA/g, (c) rate capabilities of the FeOOH/SWNT electrode

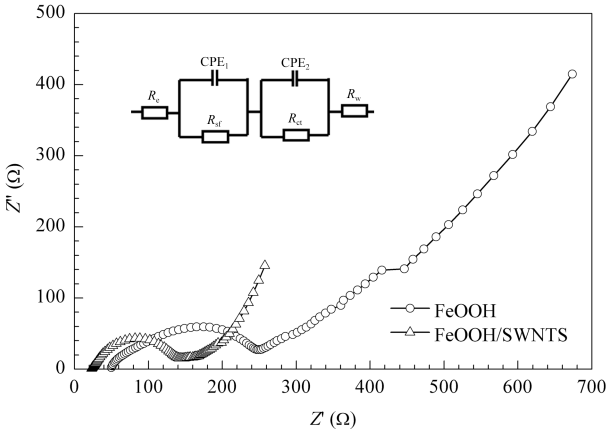

Figure 5. EIS profiles of FeOOH and FeOOH/SWNT electrodes after test. The inset shows the corresponding equivalent circuit

Table 1. Impedance parameters of FeOOH and FeOOH/SWNT electrodes after test

Electrodes	R_{e} (Ω)	R_{sf} (Ω)	R_{ct} (Ω)	$D_{\text{Li+}}$ (cm^2/s)
FeOOH	54.96	54.63	137.5	8.99×10^{-12}
FeOOH/SWNTs	25.5	93.29	24.56	3.74×10^{-11}

Figure 6 shows the linear fitting of Z_{real} vs. $\omega^{-1/2}$, from which the slope σ can be obtained, through related calculation expression can get that the $D_{\text{Li+}}$ for FeOOH/SWNT is 3.74×10^{-11} $\text{cm}^2\cdot\text{s}^{-1}$. In comparison, the diffusion coefficient for FeOOH shows a lower value of 8.99×10^{-12} $\text{cm}^2\cdot\text{s}^{-1}$. Thus, the SWNT matrix can improve the conductivity of this composite and support the FeOOH aggregation particles to alleviate the degrading of the electrode, obviously improving the electrochemical performance.

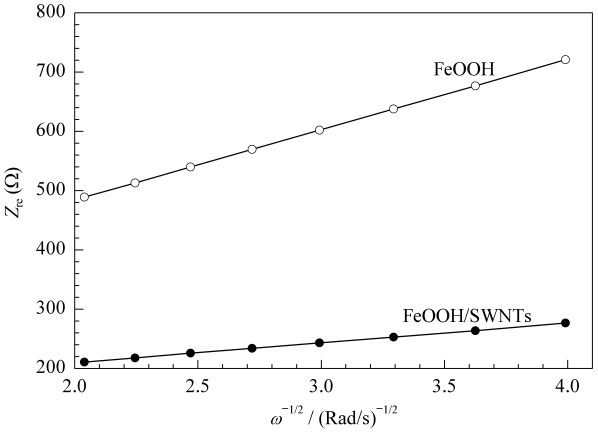

Figure 6. The linear fitting of Z_{real} vs. $\omega^{-1/2}$

4. Conclusions

In summary, a simple approach was used to fabricate FeOOH/SWNT composite in which FeOOH particles are uniformly mixed with the electric SWNT matrix. As an anode for LIBs, the FeOOH/SWNT composite demonstrated

a high reversible specific capacity, superior rate capability and outstanding cycling stability. After 180 cycles, a high reversible capacity of 758 $mAh \cdot g^{-1}$ under a current density of 400 $mA \cdot g^{-1}$ still remained, which is much higher than any other reports on FeOOH-based anodes. Thus, this FeOOH/SWNT electrode can be considered as a promising anode material for LIBs, and this proposed simple synthesis method can be readily adapted to its production on a large scale.

Acknowledgements

We thank Prof. Lunhui Guan (from FJIRSM, CAS) for his help. We acknowledge the financial support by the Natural Science Foundations of China (No.21203025, No. 11004032 and No.11074039).

References

[1] Armand M, Tarascon J M. *Nature*, 2008, 451(7179): 652
[2] Li H, Wang Z X, Chen L Q, Huang X J. *Adv Mater*, 2009, 21(45): 4593
[3] Thackeray M M, Wolverton C, Isaacs E D. *Energy Environ Sci*, 2012, 5(7): 7854
[4] Zhou G M, Wang D W, Yin L C, Li N, Li F, Cheng H M. *ACS Nano*, 2012, 6(4): 3214
[5] Zhou G M, Wang D W, Hou P X, Li W S, Li N, Liu C, Li F, Cheng H M. *J Mater Chem*, 2012, 22(34): 17942
[6] Han F, Li W C, Li D, Lu A H. *J Energy Chem*, 2013, 22(2): 329
[7] Ban C M, Wu Z C, Gillaspie D T, Chen L, Yan Y F, Blackburn J L, Dillon A C. *Adv Mater*, 2010, 22(20): E145
[8] Chen J S, Zhang Y M, Lou X W. *ACS Appl Mater Interf*, 2011, 3(9): 3276
[9] Ke F S, Huang L, Zhang B, Wei G Z, Xue L J, Li J T, Sun S G. *Electrochim Acta*, 2012, 78: 585
[10] Li J X, Zhao Y, Ding Y H, Guan L H. *RSC Advances*, 2012, 2(10): 4205
[11] Lou X M, Wu X Z, Zhang Y X. *Electrochem Comm*, 2009, 11(8): 1696
[12] Tabuchi T, Katayama Y, Nukuda T, Ogumi Z. *J Power Sources*, 2009, 191(2): 636
[13] Zhang C M, Zhu J X, Rui X H, Chen J, Sim D H, Shi W H, Hng H H, Lim T M, Yan Q Y. *Cryst Eng Comm*, 2012, 14(1): 147
[14] Funabiki A, Yasuda H, Yamachi M. *J Power Sources*, 2003, 119: 290
[15] Jain G, Capozzi C J, Xu J J. *J Electrochem Soc*, 2003, 150(6): A806
[16] Tabuchi T, Katayama Y, Nukuda T, Ogumi Z. *J Power Sources*, 2009, 191(2): 640
[17] Ren Y, Armstrong A R, Jiao F, Bruce P G. *J Am Chem Soc*, 2010, 132(3): 996
[18] Wu X L, Jiang L Y, Cao F F, Guo Y G, Wan L J. *Adv Mater*, 2009, 21(25): 2710
[19] Li J X, Wu C X, Guan L H. *J Phys Chem C*, 2009, 113(42): 18431
[20] Li J X, Zhao Y, Guan L H. *Electrochem Comm*, 2010, 12(4): 592
[21] Li J X, Zou M Z, Zhao Y, Lin Y B, Lai H, Guan L H, Huang Z G. *Electrochim Acta*, 2013, 111: 165